

Reduction of Volume Shrinkage in Holographic Polymer Dispersed Liquid Crystal Based on Epoxy Containing Polymer Matrices

Ju Yeon Woo,[1] Young Soo Kang,[2] and Byung Kyu Kim*[1]

[1]Department of Polymer Science and Engineering, Pusan National University, Busan 609-735, Korea

[2]Department of Chemistry, Sogang University, Seoul 121-742, Korea

Received February 2, 2010; E-mail: bkkim@pnu.edu

The grating formation dynamics, SEM images, diffraction efficiency, and electrooptical properties of transmission grating of holographic polymer dispersed liquid crystals (HPDLCs) have been investigated by incorporating three different types of monofunctional reactive diluents into the host polymer matrices. A gradual increase of real time diffraction efficiency, a decrease of LC droplet size, and an increase of diffraction efficiency of the composite film were obtained with the addition of epoxy acrylate monomers due to the increased viscosity of polymer/LC mixtures leading to decreased droplet coalescence. In addition, epoxy acrylate monomers induced decreased volume shrinkage according to their ring structure with bulky group. Driving voltage increased with the addition of epoxy monomers whereas rise time and decay time decreased as a result of the decreased LC droplet size. At an optimum composition of epoxy monomer, a minimum switching voltage of 6 $V\,\mu m^{-1}$ and rise time of 0.15 ms and a decay time of 18.05 ms were respectively obtained.

As a class of photoelectronic composite materials, HPDLCs are very powerful technologies for a number of electrooptical applications such as flat panel displays,[1,2] switchable lenses,[3,4] spatially patterned devices,[5] lasing,[6] information storage, and many others.[7–10]

HPDLCs are composite films containing liquid crystal (LC) and photoreactive monomer which are exposed to a coherent interference pattern generated by a holographic illumination.[11] The periodic light intensity gradient resulting from holographic exposure induces mass transport of monomer into the regions of high light intensity and nonreactive LC into the dark regions by photopolymerization induced concentration gradient and anisotropic phase separation (PIPS).[12] The morphology of HPDLCs consists of alternating layers of solid polymer and LC droplet-rich regions.[13]

The overall performance of HPDLC gratings depends strongly on the LC droplet size and shape, amount of LC phase separation, and refractive index mismatch of the polymer and LC phases.[14–17] The LC domain size and shape can be controlled by adjusting the kinetics of polymerization and phase separation of LC. Many research groups have made efforts to manipulate and improve HPDLC performance parameters such as diffraction efficiency, contrast, switching speed, and voltages. These include photocurable acrylate systems,[2–5,8,14–16,18–23] photopolymerizable thiol–ene based polymers,[11–13,24,25] partial matrix fluorination,[21,26,27] non-reactive surfactant-like molecules,[22,28,29] conductive polymer molecules,[10,30] and so on.[23,31–34] In most visibly recorded HPDLCs to date, a number of additives are typically required.[29]

Shrinkage, which mainly consists of changes in intermolecular distances[35] during polymerization, is a common and well-known problem in HPDLC materials. Polymerization shrinkage depends largely on several factors such as the nature and functionality of monomers, the structure of forming polymer chains, and the type of polymerization.[36] The shrinkage effect can significantly change the performance of HPDLCs. In particular, it is notoriously inhomogeneous, imparting blue shift, chirp, and nonsymmetric optical behavior to holographic diffraction gratings.[13] There have been numerous approaches to reduce the volume shrinkage based on thiol–ene based polymers, organic–inorganic hybrid,[37] nitroxide radicals,[38] and siloxane network formation.[17]

This report investigates the impact of polymerization behavior on LC phase separation, morphology, and electrooptical performance of HPDLCs made from epoxy acrylate based polymerizations. Epoxy acrylate presents a number of advantages including lack of inhibition by atmospheric oxygen, post-polymerization in the dark, high mechanical performance and good adhesion to various substrates. Moreover, the presence of epoxide groups in the polymer matrix of the HPDLC gratings should be more suitable to control the volume shrinkage due to their ring structure with bulky groups. We measured real time and saturation diffraction efficiency, scanning electron microscopy (SEM) images, switching voltage, and response time of the HPDLC films.

Experimental

Materials. To synthesize the poly(urethane acrylate) (PUA) oligomers, molar excess of hexamethylene diisocyanate (HDI) was reacted with bifunctional poly(propylene glycol) (PPG) ($M_n = 400\,g\,mol^{-1}$) to form isocyanate (NCO) terminated polyurethane prepolymer, followed by capping with hydroxyethyl acrylate (HEA). Detailed synthetic procedures are described in our early paper.[22,23] 2-ethylhexyl acrylate (EHA) was used as monofunctional reactive diluent. This helps to dissolve different compounds in the mixture and reduce the viscosity. Two types of epoxy acrylate viz. glycidyl methacrylate (GM), soybean oil (epoxidized acrylate (SO)) were also

Published on the web May 28, 2010; doi:10.1246/bcsj.20100030

used as monofunctional reactive diluents. Multifunctional monomer viz dipentaerythritol penta-/hexa-acrylate (DPHPA) provides the mixture with high reactivity and polymer with highly networked structure. The composition of oligomer/monofunctional/multifunctional diluents was varied 4/2/4, 4/3/3, and 4/2/4 by weight, respectively (for example, GM4/3/3 means PUA/GM/DPHPA = 4/3/3).

0.3 wt % of Rose Bengal (RB) was used as photoinitiator for holographic recording with an argon ion laser because it displays a broad absorption in the region of 450 to 560 nm and has a high triplet quantum yield.[39] To this, 1.8 wt % of *N*-phenylglycine (NPG) was added as coinitiator. The excited RB undergoes an electron-transfer reaction in which NPG functions as an electron donor, producing an NPG radical. Free radical polymerization is then initiated by the NPG radical.[7]

In addition, 6 wt % of surfactant (octanoic acid) was added to the mixture to lower the switching field. E7 (BL001, Merck), a eutectic mixture of three cyanobiphenyl and one cyanoterphenyl with high birefringence ($n_o = 1.5216$, $n_e = 1.7462$), adequate T_{NI} (61 °C) and positive dielectric anisotropy ($\Delta\varepsilon =$ 13.8) has been used as the LC at 35 wt %.

Grating Fabrication and Measurements. To fabricate holographic grating, prepolymer/LC mixture was sandwiched between two indium–tin–oxide (ITO) coated glass plates, with a gap of 10 μm which was adjusted by a bead spacer. The writing geometry is accomplished by interference of two coherent laser beams (Ar-ion laser) from a 514 nm of equal intensity with a total power of 100 mW cm^{-2} for 600 s. In this study, the external incident beam angle was fixed at 26° against the line perpendicular to the plane of the recording cell. The interference of the two beams established the periodic interference pattern and the periodicity of the polymeric structure was expressed by Bragg's law ($\Lambda = \lambda/2\sin(\frac{\theta}{2})$, Λ = grating spacing, λ = wavelength of the writing beam).

The diffraction efficiencies of the holographic gratings were measured with a photodiode using an Ar-ion laser. Diffraction efficiency is defined as the ratio of diffraction intensity after recording to transmitted beam intensity before recording. Real time grating formation was monitored using a He-Ne laser probe (633 nm) with incident angle set at the appropriate Bragg angle, since the material is not sensitive to red light. For electrooptic measurements, a square wave voltage (50 Hz sine wave pulse of 50 ms) operating from 0 to 80 V was applied across the HPDLC cell. The drive signal and the response of the photodiode were monitored with a digital storage oscilloscope (Hitachi VC-6023). The response time is defined as the time taken to relax from 90 to 10% of the maximum switching difference under an electric field. The grating morphology was visualized by scanning electron microscopy (SEM, Hitachi S430). For this, samples were prepared by freezing and fracturing the HPDLC cells in liquid nitrogen, and washed with methanol for 24 h to extract the LC. Exposed surface of the samples for SEM was coated with a thin layer of Pt–Pd to minimize artifacts associated with sample charging.

Results and Discussion

Grating Formation Dynamics. Figure 1a shows the real time diffraction efficiency as a function of irradiation time for various types of monofunctional reactive diluents. Regardless

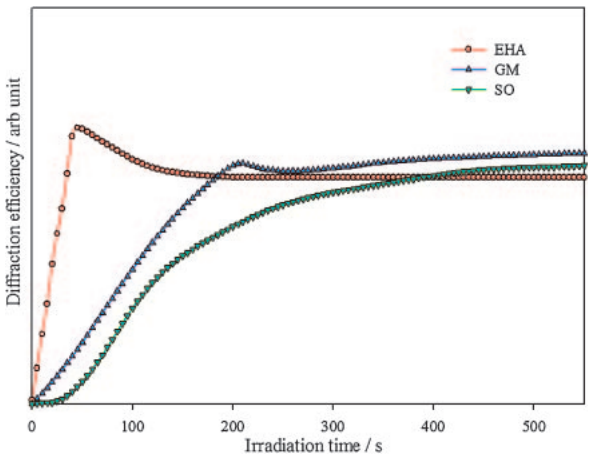

(a)

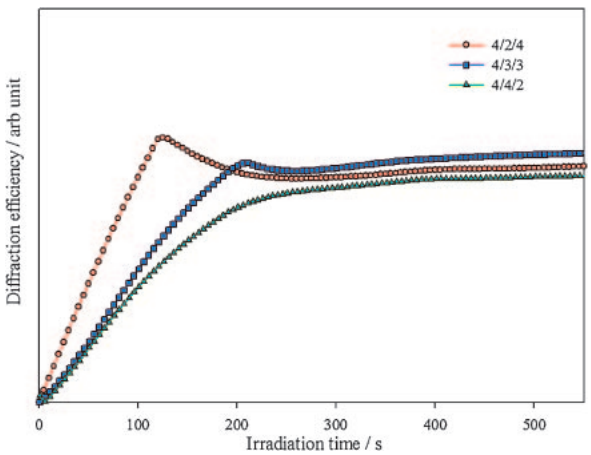

(b)

Figure 1. Real time diffraction efficiency as a function of irradiation time for various types of monofunctional reactive diluents (a) and at various compositions of GM (b) in a developing HPDLC grating (irradiated at 633 nm).

of the type of monofunctional reactive diluents, the process of grating formation shows three regions,[33] i.e., a short induction period, a period of rapid polymerization, and a plateau region. EHA shows early diffraction efficiency maximum, followed by an asymptotic decrease to a stable value. Such an early overshoot is indicative of the fast grating formation caused by the easy diffusion and the distinct phase separation due to the relatively low viscosity compared with epoxy acrylate monomer, which subsequently causes droplets to coalescence to sizes larger than the critical size of scatterings, giving rise to a decrease in diffraction efficiency. On the other hand, GM and SO do not show early overshoot and increases gradually to a saturation value. This is attributed to the slow polymerization and phase separation, which is driven by the high viscosity causing slow diffusion of LC and monomer. The slow phase separation gives difficulty in droplet coalescence, which gives little random scattering and hence high saturation efficiency. However, when the viscosity of prepolymer mixture is too high (in case of SO), diffusion becomes slower and more LC is entrapped in the polymer region leading to low diffraction efficiency.

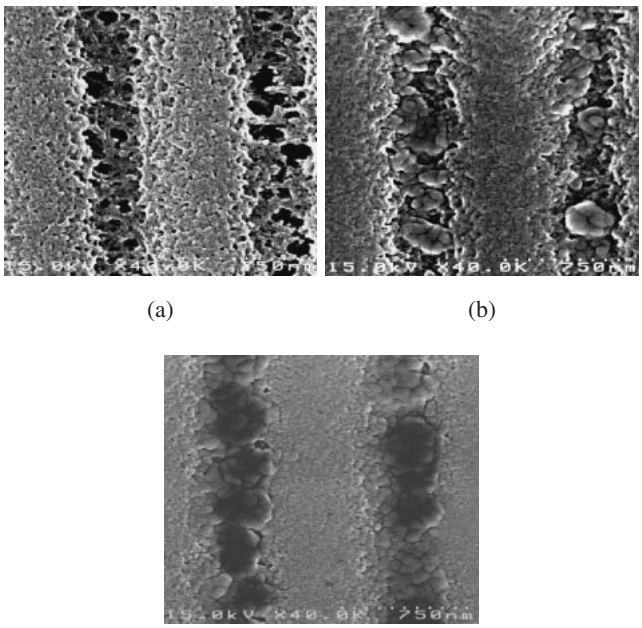

(a) (b)

(c)

Figure 2. Scanning electron microscopy (SEM) images of the transmission gratings prepared with EHA4/3/3 (a), GM4/3/3 (b), and SO4/3/3 (c).

Figure 1b shows the real time diffraction efficiency as a function of irradiation time at various compositions of GM. The increase of GM eventually decreases the average functionality of the system.[27] A fast polymerization rate following the high average functionality (GM4/2/4) leads to early overshoot and an extensive droplet coalescence, giving rise to a decrease in diffraction efficiency. On the other hand, the slow polymerization rate with low reactivity (GM4/4/2) insufficiently squeezes the LC molecules out of the polymer-rich domains, resulting in relatively low diffraction efficiency. It is seen that GM4/3/3 gives the highest real time diffraction efficiency due to the proper balance of the polymerization rate and the rate of diffusion.

SEM Images. The performance of holographic gratings in terms of diffraction efficiency, switching voltage, speeds, and background scatter are inherently related to the solid-state morphology of the grating structures.[8,40] Figure 2 shows a SEM image of the HPDLC grating as a function of the type of monofunctional reactive diluents. Grating period calculated according to Bragg's law was 1142 nm in our work. However, due to the shrinkage upon polymerization, the fabricated grating spacing is reduced. As shown in Table 1, the degree of volume shrinkage with epoxy monomers (GM and SO) is much smaller than that of EHA having no epoxy monomer. The SO4/3/3 containing the highest content of epoxide group shows the lowest volume shrinkage due to their ring structure with bulky groups. Also, droplet size increases in the order of SO < GM < EHA, which is consistent with the real time diffraction efficiency. The micrographs (Figures 2a, 2b, and 2c) clearly show that the epoxy monomers can impart significant changes in grating morphology and LC droplet size.

Figure 3 shows a SEM image of the HPDLC grating as a function of GM composition. The width of the LC-rich regions

Table 1. The Degree of Volume Shrinkage according to the Types of Monofunctional Reactive Diluents and the Composition of GM

	Average grating spacing/nm	Degree of volume shrinkage/%
EHA4/3/3	985 ± 70	13.6
GM4/3/3	1045 ± 45	8.4
SO4/3/3	1075 ± 65	5.7
GM4/2/4	1030 ± 45	9.6
GM4/4/2	1055 ± 60	7.7

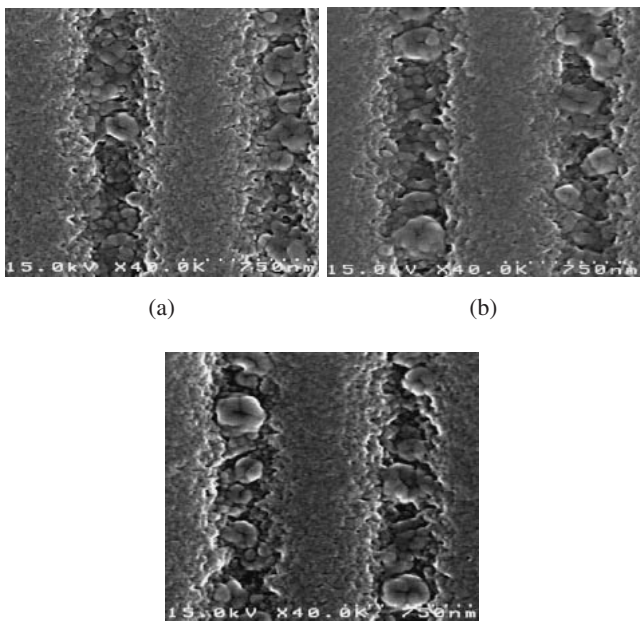

(a) (b)

(c)

Figure 3. Scanning electron microscopy (SEM) images of the transmission gratings prepared with GM4/2/4 (a), GM4/3/3 (b), and GM4/4/2 (c).

is approximately 400 nm separated by dense polymer-rich lamellas of 500–650 mm width. As monofunctional reactive diluent functionality is decreased, the width of the polymer lamellae increases. With increasing concentration of GM, the degree of volume shrinkage is reduced from 9.6 to 7.7%. This is due to the increased epoxide groups with ring structure and bulky groups. Also, it is apparent from the SEM micrographs that as the content of epoxy monomer increases, size and distribution of the nematic domains, and the LC volume fraction decrease in the transmission grating due to the low reactivity leading to the slow polymerization and phase separation.

Diffraction Efficiency. Figure 4 shows the diffraction efficiency as a function of composition of oligomer/monofunctional/multifunctional diluents for various types of monofunctional reactive diluent. As expected from the real time measurements and SEM morphology, higher diffraction efficiency is obtained with GM4/3/3. This seems reasonable since with high average monomer functionalities (GM4/2/4) highly networked acrylate domains having extremely high viscosity are quickly formed, which disturbs migration of LC and grating

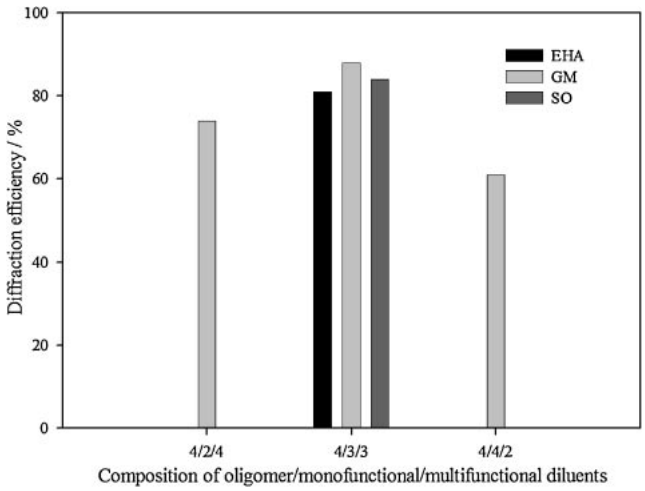

Figure 4. Diffraction efficiency as a function of composition of oligomer/monofunctional/multifunctional diluents for various types of monofunctional reactive diluents.

formation leading to lower diffraction efficiency. On the other hands, low average monomer functionalities (GM4/4/2) give narrow and poor polymer–LC phase separation leading to lower diffraction efficiency due presumably to the insufficient migration of LC molecules out of the polymer-rich regions.

With regard to the effect of types of monofunctional reactive diluents, the EHA4/3/3 shows the lowest diffraction efficiency. This implies that the rapid migration of LC molecules into the LC-rich region leads to extensive droplet coalescence to form large LC droplets due to the relatively small viscosity. This lowers droplet density and enlarges domain size leading to high scattering loss. In case of SO4/3/3, diffraction efficiency is slightly lower than that of GM4/3/3 due to the high viscosity as mentioned in real time diffraction efficiency.

Electrooptical Properties. Figure 5a shows the diffraction efficiency of the film as a function of applied voltage for various types of monofunctional reactive diluents. Switching voltage is defined as the voltage of 90% drop in diffraction efficiency. When the power is off, GM4/3/3 gives the highest diffraction efficiency of about 90%. Upon applying the voltage, diffraction efficiency decreases to a constant value of about 10% implying that LC molecules are oriented along the electric field direction and lights are transmitted. As the epoxide group increases, the switching voltage slightly increases from 5 to $6\,V\,\mu m^{-1}$ along the order of EHA < GM < SO. This is due to the decrease in the droplet size and distribution of nematic domains caused by increased viscosity, as seen in the morphology of Figure 2. Figure 5b shows the diffraction efficiency of the film as a function of applied voltage at various compositions of GM. Regardless of the compositions of GM, the switching voltage is approximately constant having a stable value of $6\,V\,\mu m^{-1}$.

Figure 6 shows rise time and decay time of HPDLC film for various applied voltage for GM4/3/3, and the response times with saturation voltage for various types of monofunctional reactive diluents are given in Table 2. The hologram is initially diffracted until the applied field realigns the liquid crystal in the droplet, thus changing the index modulation of the periodic phase grating and clearing film. Upon removal of the voltages,

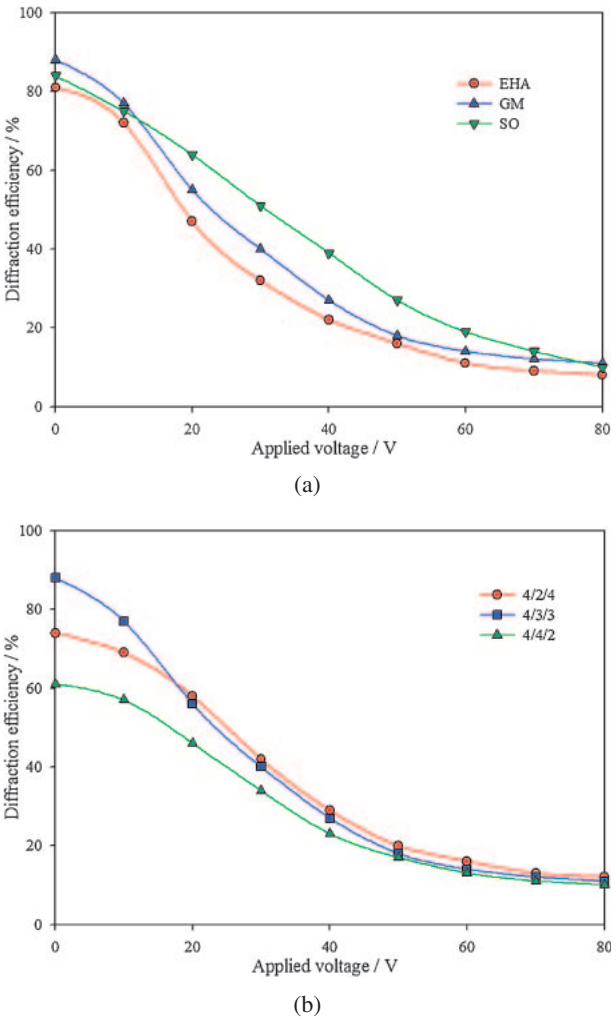

Figure 5. Diffraction efficiency as a function of applied voltage for various types of monofunctional reactive diluents (a) and at various compositions of GM (b).

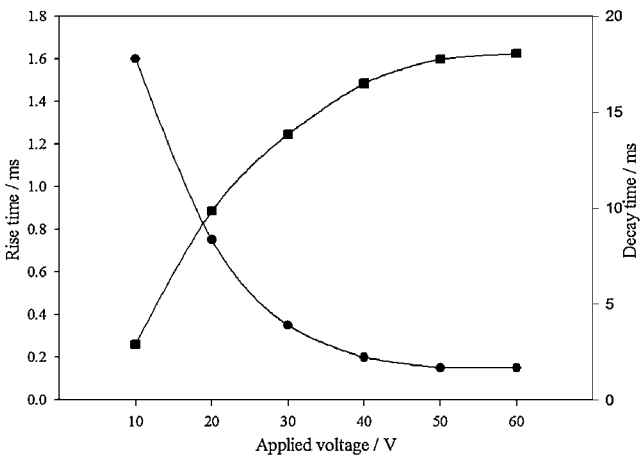

Figure 6. Rise time and decay time of HPDLC films as a function of applied voltage (GM4/3/3).

due to the inherent properties of LC (droplet size, viscosity, elastic force) and film geometry, LC molecules relax to their initial equilibrium distribution.[8] Rise time, defined as the time

Table 2. Response Time of the Film as a Function of Types of Monofunctional Reactive Diluents ($6\,V\,\mu m^{-1}$)

Response time	Types of monofunctional reactive diluents		
	EHA	GM	SO
Rise time/ms	0.25	0.15	0.15
Decay time/ms	24.80	18.05	17.85

required for the transmittance to rise from 10 to 90% in the wave form. Rise time is expected to be field dependent and rapidly decreases with increasing voltages and is less than 1 ms at saturation voltage. On the other hand, decay time shows the opposite tendency to the rise time, that is decay time increases with increasing voltages and is approximately 18 ms. This is due to the higher order of alignment of the LC molecules and the bipolar axis along the applied electric field direction. This requires much greater distortion of the director upon field removal and in turn a greater restoration energy, resulting in an overall slow relaxation process at higher voltages.[41] As the epoxide group increases, the response time decreases due to the decreased LC droplet size. For GM4/3/3, rise time of 0.15 ms and decay time 18.05 ms are obtained under the applied voltage of $6\,V\,\mu m^{-1}$.

Conclusion

Epoxy acrylate monomers have been introduced into the conventional formulation of holographic polymer dispersed liquid crystal, and the effects have been studied in terms of grating formation dynamics, morphology, volume shrinkage, diffraction efficiency, and electrooptical properties of the HPDLC films.

The addition of epoxy monomers to polymer matrices led to slow polymerization and phase separation due to the increased viscosity, This gave difficulty in droplet coalescence leading eventually to a high diffraction efficiency of the composite film, especially at a particular composition of GM4/3/3.

Also, the degree of volume shrinkage with epoxy monomers was significantly reduced due to the increased epoxide group having ring structure with a bulky group, while the droplet size increases in the order of SO < GM < EHA caused by increased viscosity.

Driving voltage increased with the addition of epoxy monomers while the rise time and decay time decreased due to the decreased LC droplet size. At an optimum composition of epoxy monomer (GM4/3/3), the degree of volume shrinkage of 8.4%, a minimum switching voltage of $6\,V\,\mu m^{-1}$ and rise time of 0.15 ms and a decay time of 18.05 ms were respectively obtained.

The research was supported by the NCRC and PNU-IFAM JRC organized at PNU.

References

1 K. Kato, T. Hisaki, M. Date, *Jpn. J. Appl. Phys.* **1999**, *38*, 1466.

2 R. L. Sutherland, L. V. Natarajan, V. P. Tondiglia, T. J. Bunning, *Proc. SPIE* **2003**, *5216*, 34.

3 L. H. Domash, Y. M. Chen, B. N. Gomatam, C. M. Gozewski, R. L. Sutherland, L. V. Natarajan, V. P. Tondiglia, T. J. Bunning, W. W. Adams, *Proc. SPIE* **1996**, *2689*, 188.

4 L. Domash, G. Crawford, A. Ashmead, R. Smith, M. Popovich, J. Storey, *Proc. SPIE* **2000**, *4107*, 46.

5 A. K. Fontecchio, M. J. Escuti, C. C. Bowley, B. Sethumadhavan, G. P. Crawford, L. Li, S. Faris, SID 2000, San Jose, CA, USA, May, **2000**, SID Digest Tech. Papers, 31, 774.

6 R. Jakubiak, T. J. Bunning, R. A. Vaia, L. V. Natarajan, V. P. Tondiglia, *Adv. Mater.* **2003**, *15*, 241.

7 J. Qi, G. P. Crawford, *Displays* **2004**, *25*, 177.

8 R. T. Pogue, R. L. Sutherland, M. G. Schmitt, L. V. Natarajan, S. A. Siwecki, V. P. Tondiglia, T. J. Bunning, *Appl. Spectrosc.* **2000**, *54*, 12A.

9 H. S. Nalwa, *Handbook of Advanced Electronic and Photonic Materials and Devices*, Academic Press, San Diego, **2001**.

10 F. P. Nicoletta, G. Chidichimo, D. Cupelli, G. D. Filpo, M. D. Benedittis, B. Gabriele, G. Salerno, A. Fazio, *Adv. Funct. Mater.* **2005**, *15*, 995.

11 A. F. Senyurt, G. Warren, J. B. Whitehead, Jr., C. E. Hoyle, *Polymer* **2006**, *47*, 2741.

12 T. J. White, L. V. Natarajan, V. P. Tondiglia, P. F. Lloyd, T. J. Bunning, C. A. Guymon, *Polymer* **2007**, *48*, 5979.

13 T. J. White, L. V. Natarajan, V. P. Tondiglia, P. F. Lloyd, T. J. Bunning, C. A. Guymon, *Macromolecules* **2007**, *40*, 1121.

14 J. Y. Woo, E. H. Kim, B. K. Kim, *ChemPhysChem* **2008**, *9*, 141.

15 K. Beev, L. Criante, D. E. Lucchetta, F. Simoni, S. Sainov, *Opt. Commun.* **2006**, *260*, 192.

16 J. He, B. Yan, B. Yu, S. Wang, Y. Zeng, Y. Wang, *Eur. Polym. J.* **2007**, *43*, 2745.

17 Y.-Y. Liao, J.-H. Liu, *React. Funct. Polym.* **2009**, *69*, 281.

18 I. Drevenšek-Olenik, M. Jazbinšek, M. E. Sousa, A. K. Fontecchio, G. P. Crawford, M. Čopič, *Phys. Rev. E: Stat., Nonlinear, Soft Matter Phys.* **2004**, *69*, 051703.

19 M. De Sarkar, N. L. Gill, J. B. Whitehead, G. P. Crawford, *Macromolecules* **2003**, *36*, 630.

20 T. J. White, C. A. Guymon, *Polym. Mater. Sci. Eng.* **2003**, *89*, 452.

21 E. H. Kim, J. Y. Woo, Y. H. Cho, B. K. Kim, *Bull. Chem. Soc. Jpn.* **2008**, *81*, 773.

22 J. Y. Woo, B. K. Kim, *ChemPhysChem* **2007**, *8*, 175.

23 J. Y. Woo, E. H. Kim, B. K. Kim, Y. H. Cho, *Liq. Cryst.* **2007**, *34*, 527.

24 L. V. Natarajan, C. K. Shepherd, D. M. Brandelik, R. L. Sutherland, S. Chandra, V. P. Tondiglia, D. W. Tomlin, T. J. Bunning, *Chem. Mater.* **2003**, *15*, 2477.

25 N. B. Cramer, C. N. Bowman, *J. Polym. Sci., Part A: Polym. Chem.* **2001**, *39*, 3311.

26 M. D. Schulte, S. J. Clarson, L. V. Natarajan, D. W. Tomlin, T. J. Bunning, *Liq. Cryst.* **2000**, *27*, 467.

27 M. De Sarkar, J. Qi, G. P. Crawford, *Polymer* **2002**, *43*, 7335.

28 J. Klosterman, L. V. Natarajan, V. P. Tondiglia, R. L. Sutherland, T. J. White, C. A. Guymon, T. J. Bunning, *Polymer* **2004**, *45*, 7213.

29 Y. J. Liu, X. W. Sun, H. T. Dai, J. H. Liu, K. S. Xu, *Opt. Mater.* **2005**, *27*, 1451.

30 D. Cupelli, F. P. Nicoletta, G. De Filpo, G. Chidichimo, A. Fazio, B. Gabriele, G. Salerno, *Appl. Phys. Lett.* **2004**, *85*, 3292.

31 W. Li, H. Zhang, L. Wang, C. Ouyang, X. Ding, H. Cao, H.

Yang, *J. Appl. Polym. Sci.* **2007**, *105*, 2185.
32 Y. H. Cho, M. He, B. K. Kim, Y. Kawakami, *Sci. Technol. Adv. Mater.* **2004**, *5*, 319.
33 T. J. Bunning, L. V. Natarajan, V. P. Tondiglia, R. L. Sutherland, *Annu. Rev. Mater. Sci.* **2000**, *30*, 83.
34 H. Ono, A. Hatayama, A. Emoto, N. Kawatsuki, *Thin Solid Films* **2008**, *516*, 4178.
35 M. Dewaele, D. Trufier-Boutry, G. Leloup, J. Devaux, *Eur. Cell. Mater.* **2005**, *9*, Suppl. 1, 66.
36 S. P. Papps, *Radiation Curing Science and Technology*, Plenum Press, New York, **1992**.
37 W. S. Kim, Y.-C. Jeong, J.-K. Park, *Appl. Phys. Lett.* **2005**, *87*, 012106.
38 R. Castagna, F. Vita, D. E. Lucchetta, L. Criante, L. Greci, P. Ferraris, F. Simoni, *Opt. Mater.* **2007**, *30*, 539.
39 P. S. Drzaic, *Liquid Crystal Dispersions*, World Scientific, Singapore, **1995**.
40 Y. M. Huang, L. Chen, *Thin Solid Films* **2006**, *515*, 2026.
41 A. K. Kalkar, V. V. Kunte, S. A. Bhamare, *J. Appl. Polym. Sci.* **2008**, *107*, 689.